SYNCHROTRON X-RAY POWDER DIFFRACTION AT GILDA

REPORT ON EXPERIMENTS 08-02-155 AND 08-02-174

Roberto Millini*, Donatella Berti and Danila Ghisletti
Physical-Chemistry Dept. EniTecnologie S.p.A.
Via F. Maritano 26, I-20097 San Donato Milanese (MI -Italy)
e-mail: rmillini@enitecnologie.eni.it

Experiment 08-02.155: Structural Characterization of Microporous Titanium-Silicates Precursors (01.10.98 - 05.10.98)

Experiment 08-02-174: Structural Characterization of Zeolite Precursors (15.02.99 - 17.02.99)

1. INTRODUCTION

The isomorphous substitution of Al and/or Si by other tri- and tetravalent elements in the framework structure of zeolites is a well recognized method for producing materials with novel catalytic properties. Several authors have claimed the possibility of incorporating a large number of elements in framework positions, but only a few (B [1], Ga [2], Fe [3], V [3] and Ti [3]) have been proved, leading to the formation of microporous materials with catalytic properties different from those of the parent aluminosilicates. In particular, the incorporation of Ti in the MFI framework, achieved in the ENI laboratories, represents the most successful result in this field owing to the remarkable catalytic activity of Titanium-Silicalite-1 (TS-1) in oxidation reactions of organic substrates (e.g. aromatics, olefins) with H_2O_2 [4]. Another interesting result, obtained again in the ENI laboratories, is represented by the synthesis of BOR-C, a microporous borosilicate with the MFI framework structure [5]. Substitution of Al by B can be considered as an effective way for modifying the acidic properties of zeolites in view of practical applications in acid-catalyzed reactions requiring low acidic strength. The catalytic performances of these materials are strongly related to the effective incorporation of the heteroatom (Ti, B) in the zeolite framework which is however limited to a few percent concentration. In fact, in the case of TS-1 the maximum concentration achievable is ca. 2.5 atoms % [6], while in BOR-C is ca. 4 atoms % [1,5]. This makes the characterization of these materials difficult and requires the use of a large number of physico-chemical techniques [1,3]. Definitive proofs supporting the real incorporation of B and Ti have been obtained by X-ray powder diffraction [1,3]. Till now the attention has been devoted to the characterization of the calcined material, while no information exists about the structural characteristics of the as-synthesized materials (i.e. the materials containing the organic molecules (tetrapropylammonium ions) acting as structure-directing agents (SDA) in the zeolite crystallization). This information could be

fundamental for better understanding the role of SDA in molecular sieve formation and for evaluating the reasons of the low extent of isomorphous substitution.

The low resolution of the standard XRD equipments and the complexity of the MFI structure strongly limit the possibility to perform an accurate structural characterization of TS-1. The availability of high resolution diffraction data is a necessary starting point for better characterize these materials.

2. EXPERIMENTAL

2.1 Samples

Pure silica (S1) and Titanium-containing (TS-1) MFI samples with variable SiO_2/TiO_2 molar ratios were synthesized at 443 K from alkali free reaction mixtures according to the original recipe [7]. BOR-C sample with variable amounts of B were synthesized from alkali free reaction mixtures at 443 K following the synthesis of Taramasso et al. [5]. The list of samples with the corresponding chemical composition is reported in Table 1. For the sake of clarity, the TS-1 and BOR-C samples will be indicated with the letters T and B followed by the number of Ti and B atoms per unit cell in parentheses.

Table 1

Chemical composition[a] of the as-synthesized samples.

Sample	Chemical composition	x = [M]/[M]+[Si]	
		M = Ti	M = B
S1	$4.40TPA{\cdot}96SiO_2$	------	------
T(0.74)	$4.33TPA{\cdot}0.74TiO_2{\cdot}95.26SiO_2$	0.0077	------
T(0.98)	$4.37TPA{\cdot}0.98TiO_2{\cdot}95.02SiO_2$	0.0102	------
T(1.67)	$4.63TPA{\cdot}1.67TiO_2{\cdot}94.33SiO_2$	0.0174	------
T(1.83)	$4.25TPA{\cdot}1.83TiO_2{\cdot}94.17SiO_2$	0.0189	------
T(2.14)	$4.28TPA{\cdot}2.14TiO_2{\cdot}93.86SiO_2$	0.0223	------
B(0.70)	$4.23TPA{\cdot}0.70BO_2{\cdot}95.30SiO_2$	------	0.0073
B(1.28)	$4.51TPA{\cdot}1.28BO_2{\cdot}94.72SiO_2$	------	0.0133
B(1.90)	$4.14TPA{\cdot}1.90BO_2{\cdot}94.10SiO_2$	------	0.0199
B(3.04)	$4.20TPA{\cdot}3.04BO_2{\cdot}92.96SiO_2$	------	0.0317

[a] Ti and B contents were determined by ICP-AES (Thermo Jarrel Ash spectrometer); SiO_2 was determined gravimetrically; quantitative C, H and N analyses were carried out with a Perkin Elmer 2400 analyzer.

2.2 Synchrotron X-Ray Diffraction (SXPD)

The experiment **08-02.155** focused only on the as-synthesized TS-1 samples.

The diffraction data were collected at room temperature on samples sealed in Lindemann-glass capillary (ϕ = 1 mm) in the $3.5 \leq 2\theta \leq 35°$ angular region, with 0.01° 2θ step size and accumulation time varying between 5 and 10 s/step. These relatively long accumulation times were necessary because the synchrotron operated at the 16-bunch mode. The wavelength (0.8265 Å) was determined by using Si (SRM640b, a = 5.43094(3) Å) as an external standard.

During the experiment **08-02-174** the synchrotron operated at 2/3 filling mode. Synchrotron X-ray diffraction (SXPD) data were collected at room temperature on samples loaded in Lindemann capillaries (0.3 mm internal diameter). The beamline was set to deliver a wavelength of λ = 0.82714(2) Å, calibrated with LaB_6 (NIST/SRM660, a = 4.15690(5) Å), and collimated by two mirrors located before and after the double-crystal Si(311) and Si(511) monochromator. The capillaries were mounted on the ϕ axis of the two-circle diffractometer and axially rotated at 1 Hz during the data collection in Debye-Scherrer geometry. The whole diffraction rings were recorded on a Fuji Image Plate (IP) located at 204.83 mm from the sample and perpendicular to the incident beam (typical exposure times 2 to 3 min). The elaborations of the scanned digital images (Fuji BAS2000 scanner) were carried out with the Fit2d software package [8]. The diffraction rings were radially integrated and the intensities were corrected for flat plate geometrical distortion and polarization (polarization factor = 0.96). The intensity data were finally interpolated to fixed angular steps of 0.028452° 2θ and converted into a conventional diffracted intensity vs. diffraction angle profile, covering the $3.5 \leq 2\theta \leq 56°$ angular range.

2.3 Rietveld Analysis

Rietveld refinements of the SXPD patterns of the as-synthesized samples were carried out with the GSAS software package [9]. Two structure models of the as-synthesized MFI were initially considered: the ordered model proposed by Baerlocher, refined from X-ray powder diffraction data [10] and the disordered model reported by van Koningsveld et al. derived from single crystal X-ray diffraction data [11]. The second model gave the best fitting of the SXPD pattern of the as-synthesized S1. It was successively used for the Rietveld refinement of all the other patterns. The data below 6° 2θ (for step-scanning data) 10° 2θ (for IP data) were excluded from the refinement because of the asymmetry of the reflections. The pseudo-Voigt peak profile function, with up to 17 refinable parameters was chosen and the peaks were truncated at 0.01% of the peak maxima. Background intensity was modeled by a Chebyshev type I polynomial function with 16 - 20 background parameters. Atomic coordinates, isotropic thermal parameters and occupancy factors were kept fixed during the refinements, while scale factor, 2θ-zero point and unit cell parameters were refined. Refinement were considered converged when the sum of the ratios parameter shifts/parameter estimated standard deviation (e.s.d.) was less than 0.1.

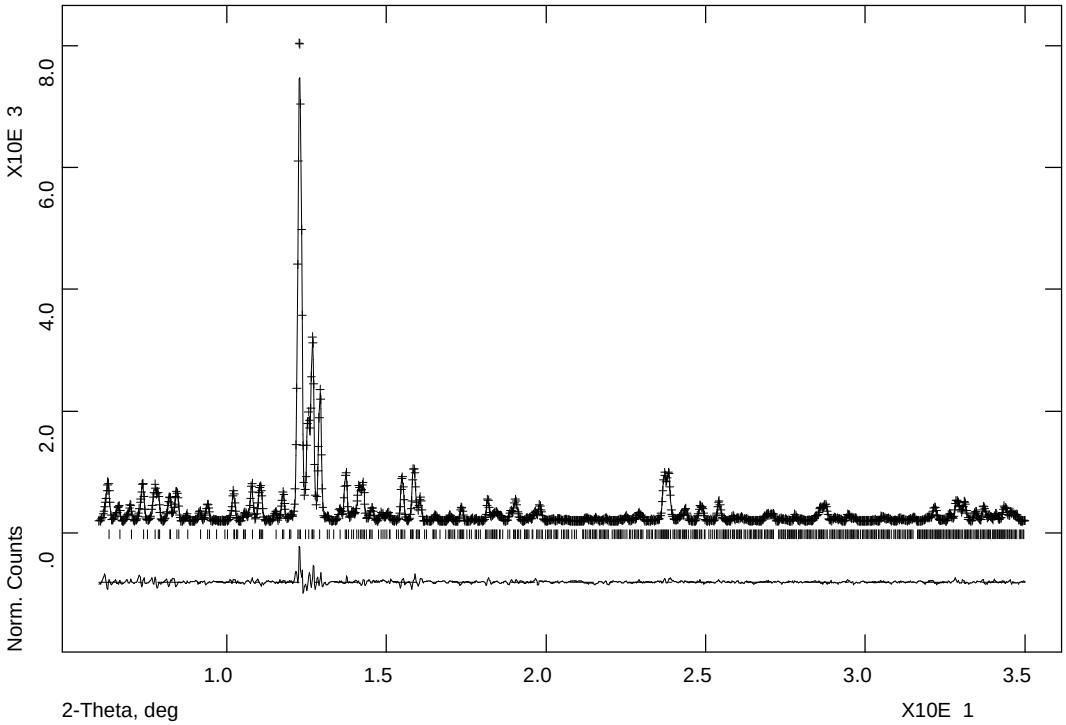

Fig. 1: Experimental (++), calculated (—) and difference (lower) SXPD patterns of sample S1 collected with the step-scanning procedure (Rp = 0.0467, wRp = 0.0675). Vertical bars indicate the positions of the 1710 Bragg reflections.

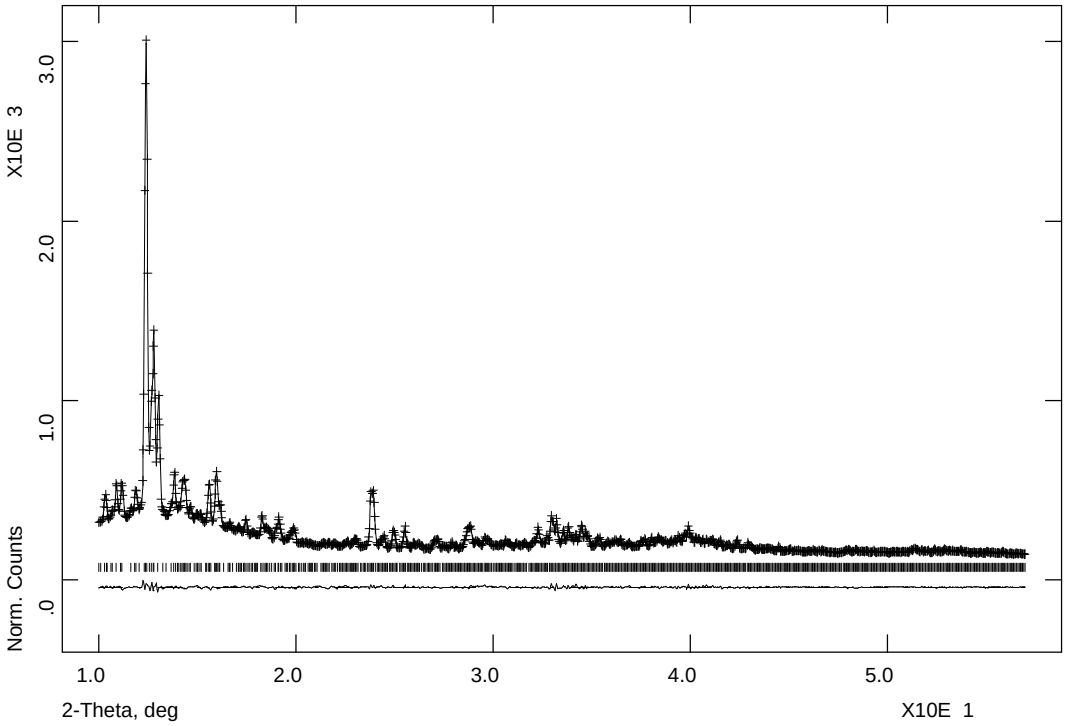

Fig. 2: Experimental (++), calculated (—) and difference (lower) SXPD patterns of sample S1 collected with the IP (R_p = 0.0090, wR_p = 0.0129). Vertical bars indicate the positions of the 4727 Bragg reflections.

3. RESULTS AND DISCUSSION

3.1 Step-scanning vs. IP data collection

Before describing the results of the refinements, it is useful to make a comparison between the data collected with the two different procedures described in the experimental section. To do that, we focus the attention on the SXPD data collected on the S1 sample, provided that all the considerations made below are valid also for all data collected on the TS-1 samples under investigation.

As clearly show in Fig. 1, refinement of the S1 powder pattern collected with the step-scanning procedure led to a good fitting of the experimental pattern as demonstrated by the relatively low values of the disagreement factors (Fig. 1). The higher discrepancies are observed in the low angular region, and are due to the high asymmetry of the reflections, only partially corrected during the refinement.

Significantly better is the fit of the experimental pattern collected with the IP (Fig. 2). The resolution of the SXPD pattern is very high even in the high angular region which was included in the refinement: that allowed to exclude from the refinement the reflections located in the region below 10° 2θ, characterized by a significant asymmetry. The final disagreement factors are unusually low (Fig. 2), demonstrating the high quality of the refinement.

In spite of these differences, the desired crystallographic data (unit cell parameters and volume) were quite similar:

Step-scan data: a = 20.0392(9), b = 19.9339(9), c = 13.4066(6) Å, V = 5355.4(3) Å^3

IP data: a = 20.0402(6), b = 19.9348(6), c = 13.4074(5) Å, V = 5356.2(2) Å^3

Table 2

Crystallographic data (e.s.d's in parentheses).

Sample	x[i]	a (Å)	b (Å)	c (Å)	V (Å^3)
S1	0.0000	20.0402(6)	19.9348(6)	13.4074(5)	5356.2(2)
T(0.74)	0.0077	20.0532(6)	19.9491(6)	13.4123(5)	5365.5(2)
T(0.98)	0.0102	20.0599(6)	19.9545(6)	13.4139(5)	5369.4(2)
T(1.67)	0.0174	20.0720(6)	19.9649(6)	13.4195(5)	5377.7(2)
T(1.83)	0.0189	20.0741(6)	19.9699(6)	13.4203(5)	5379.9(2)
T(2.14)	0.0223	20.0820(6)	19.9788(6)	13.4232(5)	5385.6(2)
B(0.70)	0.0073	20.0282(6)	19.9159(6)	13.3897(5)	5340.9(2)
B(1.28)	0.0133	20.0238(6)	19.9042(6)	13.3819(5)	5333.5(2)
B(1.90)	0.0199	20.0101(6)	19.8857(6)	13.3635(5)	5317.5(2)
B(3.04)	0.0317	19.9955(6)	19.8582(6)	13.3391(5)	5296.6(2)

[i] x = [M]/[M] + [Si] (M = Ti, B), from elemental analysis

3.2 Refinement of SXPD patterns of as -synthesized TS-1 and BOR-C samples

Refinement of the SXPD patterns of as-synthesized S1, TS-1 and BOR-C samples led to the results reported in Table 2.

First of all, a comment is necessary for the pure silica MFI structure (sample S1). Compared with the calcined sample, the unit cell volume of the as-synthesized one is significantly higher (V = 5339.8(8) $Å^3$ [6] and 5356.2(4) (Table 2), respectively). This difference was confirmed by the Rietveld refinement of two different sets of XRD data collected on the same S1 sample (using a Philips X'PERT diffractometer and CuKα radiation) and on another S1 sample synthesized some years ago and stored in our laboratories. For this sample, the XRD data were collected on a Philips PW1710 diffractometer using CuKα radiation. The results obtained, reported in Table 3, vary within the experimental error and confirm the expansion of the lattice in the as-synthesized MFI with respect to the calcined form.

Table 3

Comparison among the crystallographic data for as-synthesized and calcined Silicalite-1 reported in the literature and in this work

Sample	a (Å)	b (Å)	c (Å)	α (°)	V ($Å^3$)	Ref.
S1	20.0402(6)	19.9348(6)	13.4075(4)	----	5356.2(2)	[i]
S1	20.0415(9)	19.9331(9)	13.4064(7)	----	5355.7(5)	[ii]
S1	20.039(3)	13.935(2)	13.406(1)	----	5355.4(10)	[iii]
S1 Calc.	20.101(1)	19.877(1)	13.365(1)	90.61(2)	5339.4(8)	[6]

[i] This work.

[ii] Rietveld refinement performed on the data collected in the $20 \leq 2\theta \leq 50°$ angular region with a Philips X'PERT diffractometer, using CuKα radiation.

[iii] Rietveld refinement performed on data collected in the $20 \leq 2\theta \leq 50°$ angular region with a Philips PW 1710 diffractometer, using CuKα radiation, on a different S1 sample.

Considering the Ti-containing samples, the results confirm the expected lattice expansion due to the substitution of Si by the larger Ti ion. As in the case of the calcined materials [6], the unit cell volume follows a Vegard's type law (see the linear regression equations reported in Table 4), but the angular coefficient of the equation which relates the unit cell volume to the Ti content is significantly lower than the corresponding value reported for the calcined samples (Table 4). Application of the well known equation relating the unit cell volume (V_x) of a sample containing x molar fraction of heteroatom M to that of the pure silica parent structure (V_{si}):

$$V_x = V_{Si} - V_{si}[1 - (d_{M\text{-}O}/d_{Si\text{-}O})^3]x \qquad (1)$$

where $d_{M\text{-}O}$ and $d_{Si\text{-}O}$ are the tetrahedral M-O and Si-O (= 1.61 Å) bond distances, a apparent Ti-O bond distance of 1.73 Å is obtained, compared to the value of 1.80 Å computed for the calcined samples [6]. It is evident that the additional lattice volume

required for Ti incorporation is partly supplied by the expansion caused by the occluded TPA ions.

Fig. 3 compares the unit cell volume variation determined for as-synthesized TS-1 and calcined samples. The intersection between the two straight lines occurs at x ~ 0.02. It is hypothesized, but not demonstrated here because of the difficulty to control the framework Ti content in this region, that above this value the lattice expansion of the as-synthesized samples follows that of the calcined ones. In other words, it is probable that above this limit the effect of Ti incorporation prevails over that of the TPA ions.

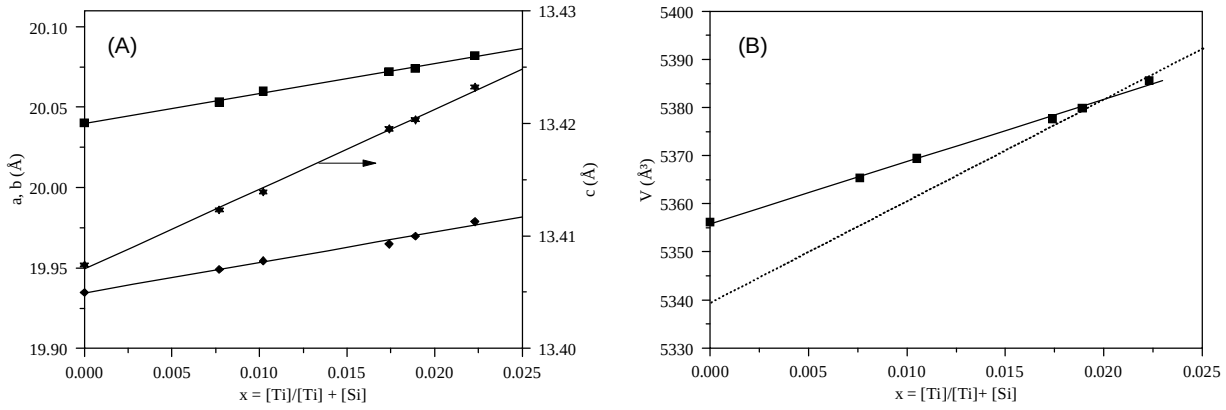

Fig. 3: (A) Variation of a (■), b (◆) and c (✱) of TS-1 as a function of Ti content.
(B) Comparison between the variation of the unit cell volume of as-synthesized (■) and calcined TS-1 samples (·····).

When considering the as-synthesized BOR-C samples, the opposite situation is observed. As in the case of the calcined samples, the replacement of Si by B induces a progressive contraction of the unit cell parameters (Fig. 4). When equation (1) is applied to the values of unit cell volume reported in Table 4, a d_{B-O} of 1.39 Å is computed. This is surprisingly low when compared with the average B-O bond distance (1.46 Å) observed in $NaBSi_3O_8$ [12] and with the corresponding d_{B-O} value of 1.44 Å derived from XRD analysis of calcined BOR-C samples [5]. Since there are no reasons to expect a contraction of the B-O bond length, the low d_{B-O} value derived for as-synthesized BOR-C can only be ascribed to a contraction of the Si-O-Si(B) angles, probably favored by coulombic interactions between the negatively charged framework and TPA cations.

The influence of the Si-O-M angles on the apparent d_{M-O} bond distance computed with equation (1) has already been observed. Ga-SOD, contrary to expectations based on the larger tetrahedral Ga-O bond distance compared to Al-O, has a smaller unit cell than the parent aluminosilicate [13]. A contraction of the Si-O-Si(B) angles in as-synthesized BOR-C samples seems to be favored by the fact that the orthorhombic MFI framework is more strained than the monoclinic one [14]. In fact, in the latter modification the Si-O-Si angles are in the range 141.3(2)-169.0(3)° (average: 147.1 - 158.8°) while in the orthorhombic framework are in the range 144.9(3) - 175.9(4)° (average: 150.5 - 162.8°).

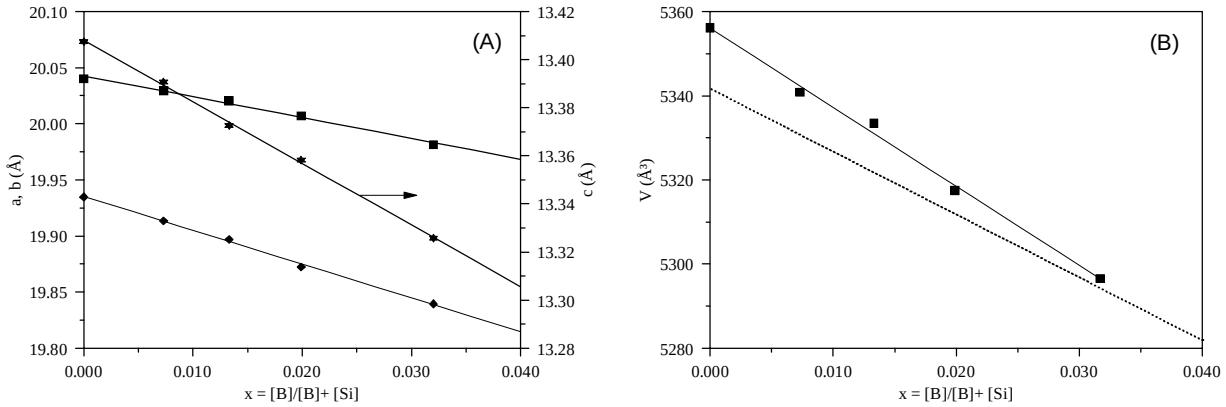

Fig. 4: (A) Variation of a (■), b (♦) and c (✱) of BOR-C as a function of B content. (B) Comparison between the variation of the unit cell volume of as-synthesized (■) and calcined BOR-C samples (···).

Table 6

Linear regression analysis of unit cell parameters[i]

	TS-1			BOR-C		
	u	v	r	u	v	r
As-synthesized						
a	1.8529	20.0399	0.9970	-1.4129	20.0420	-0.9948
b	1.8932	19.9345	0.9908	-2.4135	19.9346	-0.9993
c	0.7102	13.4070	0.9974	-2.1463	13.4073	-0.9973
V	1294.1	5355.8	0.9972	-1877.4	5356.0	-0.9977
Calcined samples[ii]						
a	1.429	20.098	0.9868	-2.709	20.107	-0.9778
b	2.975	19.882	0.9924	-1.587	19.864	-0.9144
c	2.281	13.363	0.9957	-0.896	13.375	-0.8985
V	2110.4	5339.4	0.9993	-1496.0	5341.7	-0.9924

[i] According to the equation: $y = ux + v$; r, correlation coefficient.

[ii] Data from ref. [6] for TS-1 samples and from ref. [5] for BOR-C samples.

Significant differences exist among the linear regression equations computed for the as-synthesized BOR-C samples and for the calcined ones (Table 4). However, the crystallographic data of the latter samples may be affected by some uncertainties because of the possible deboronation effects induced by the thermal treatments necessary for eliminating the TPA ions.

The equations which relate the unit cell volume variation as a function of the Ti and B content can be quantitatively used for assessing the real framework composition of the as-synthesized TS-1 and BOR-C samples and, when compared

with the same data derived from the calcined ones, for evaluating possible variations of the framework composition due to the thermal treatments.

4. CONCLUSIONS

The presence of TPA ions within the MFI pores strongly influences the structural characteristics of the as-synthesized materials. In the case of the pure silica parent structure, a significant increase in unit cell parameters and volume with respect to the calcined sample was observed, as a consequence of the intermolecular non-bonding interactions between terminal methyl groups of the propyl chains. Incorporation of Ti and B induces the expected linear lattice expansion and contraction, respectively. However, when compared with the corresponding calcined materials, significant differences were observed. In particular, the apparent tetrahedral Ti-O and B-O bond distances (d_{Ti-O} and d_{B-O}), computed with equation (1), are shorter than expected. In both cases an influence by TPA ions can be hypothesized. In TS-1 the lattice expansion induced by the organic cations partially compensates the effect of the Si substitution by the larger Ti ions. On the contrary, in the case of BOR-C, it is plausible to conclude that the coulombic interactions between TPA ions and the negatively charged framework strongly contribute to the lattice contraction. The incorporation of B mainly affects the *b* and *c* parameters, along which large Si-O-SI(B) angles (close to 180°) are found. Therefore, it is plausible that the lattice contraction is due to both the smaller B atoms and a decrease in the Si-O-Si(B) angles.

The regression curves which relate the unit cell volume variation with the Ti and B content can be usefully applied for determining the real framework composition of the as-synthesized materials, necessary for evaluating possible loss of framework Ti and B during the thermal treatments necessary for eliminating the TPA ions.

ACKNOWLEDGMENTS

The authors are grateful to S. Mobilio for the beam time at GILDA, to A. Balerna and C. Meneghini for the excellent technical assistance in the data collection and to G. Artioli and P. Norby for having provided the use of the Image Plate.

5. REFERENCES

[1] R. Millini, G. Perego, G. Bellussi, *Top. Catal.* 9 (1999) 13.

[2] R. Szostak, *Molecular Sieves. Principles of Synthesis and Identification*. Van Nostrand Reinhold, New York, 1989, p. 212.

[3] G. Perego, R. Millini, G. Bellussi, in: H. G. Karge, J. Weitkamp (Eds.), *Molecular Sieves - Science and Technology*. Vol. 1; Synthesis, Springer Verlag, Heidelberg (BRD), 1998, p. 187.

[4] G. Perego, G. Bellussi, C. Corno, M. Taramasso, F. Buonomo and A. Esposito, *Proc. 7th Int. Zeolite Conf.*, Tokyo, 1986, Elsevier, Amsterdam, 1987, p. 129.
[5] M. Taramasso, G. Perego, B. Notari, in: L. V. C. Rees (Ed.), *Proc. 5th Int. Conf. on Zeolites*, Naples, 1980, Heyden, London, 1980, p. 40.
[6] R. Millini, E. Previde Massara, G. Perego, G. Bellussi, J. Catal. 137 (1992) 497.
[7] M. Taramasso, G. Perego, B. Notari, *US Patent* 4,410,501 (1983).
[8] A.P. Hammerslay, S.O. Svensson, M. Hanfland, A.N. Fitch, D. Häusermann, *High Pressure Res.* 14 (1996) 235.
[9] A.C. Larson, R.B. Von Dreele, *GSAS. Generalized Structure Analysis System.* Document LAUR 87-748, Los Alamos National Laboratory, USA, 1994.
[10] C. Baerlocher, in: D. Olson, A. Bisio (Eds.), *Proc. 6th Int. Zeolite Conf.*, Reno, 1983, Butterworths, Guilford (UK), 1984, p. 823.
[11] H. van Koningsveld, H. van Bekkum, J.C. Jansen, *Acta Cryst.* B43 (1987) 127.
[12] D. E. Appleman, J. R. Clark, *Am. Mineral.* 50 (1965) 1827.
[13] J.M. Newsam, D.E.W. Vaughan, *Proc. 7th Int. Zeolite Conf.*, Tokyo, 1986, Elsevier, Amsterdam, 1987, p. 457.
[14] H. van Koninsgveld, J.C. Jansen, H. van Bekkum, *Zeolites* 10 (1990) 235.

LIST OF PUBLICATIONS

[1] *Structural Characterization of As-Synthesized B- and Ti-Containing MFI-Type Molecular Sieves*
Roberto Millini*, Giovanni Perego, Donatella Berti, Wallace O. Parker Jr., Angela Carati and Giuseppe Bellussi, *Microporous Mesoporous Materials* (1999) in press. (Paper reviewed).

[2] *Towards the Rational Synthesis of Zeolites*
Roberto Millini, invited lecture at the *European Research Conference*: *Chemistry and Physics of Multifunctional Materials: Taming Molecular Complexity*, San Feliu de Guixols, Spain, 21-26 Sept. 1999